High Resolution Imaging using 325 GHz and 1.5 THz Transceivers

Jason C. Dickinson, Thomas M. Goyette, and Jerry Waldman

Submillimeter-Wave Technology Laboratory
University of Massachusetts Lowell
175 Cabot St.
Lowell, MA 01854

ABSTRACT

The Submillimeter-Wave Technology Laboratory (STL) at the University of Massachusetts Lowell has designed and constructed two high resolution terahertz imaging systems based on 325 GHz and 1.5 THz transceivers. While the systems were originally designed to acquire radar signatures of high fidelity scale models, their high sensitivity and high stability at 325 GHz and 1.5 THz make them novel systems for demonstrating the imagery capabilities of terahertz rays. Unlike many terahertz detection systems, the imaging system described here uses ultra stable CO_2 pumped far-infrared (FIR) lasers to produce nominally 100 milliwatt continuous wave (CW) terahertz beams. Custom CO_2 and FIR laser designs have produced systems with extremely stable power output and low phase drift. The imagery generated by these systems is formed by full beam illumination of the target of interest, followed by coherent processing of the backscattered signal. Several terahertz images will be presented, including high resolution imagery of a concealed weapon, detected through clothing from a distance of 25 meters for each system. An image collection time of less than three minutes produced 512 x 512 pixel image with 1 to 2 mm resolution. The overall systems, including the generation of the 325 GHz and 1.5 THz beams, heterodyne detection systems, target positioning apparatus, and image formation algorithms will be discussed.

Keywords: Terahertz, THz, Imagery, Security, Concealed weapon.

1. INTRODUCTION

For the past twenty years the Submillimeter Wave Technology Laboratory (STL) at the University of Massachusetts Lowell has performed radar signature measurements of physical scale models of tactical vehicles. Currently STL and the Expert Radar Signature Solutions (ERADS) consortium have six compact radar ranges spanning frequencies from several gigahertz up to 1.6 terahertz. Two of the laser based systems located at STL will be discussed.

The earliest work in simulating full-scale radar measurements involved the use of a carbon dioxide laser, optically pumping a far-infrared (FIR) laser cell, to produce frequencies in the terahertz[1]. Bolometric detectors were used to measure the amplitude of the scatter from complex targets.

Over a decade ago, bolometric detectors were replaced with corner-cube mounted, Schottky diode heterodyne mixers in a new 1.56THz system[2]. The prototype system was replaced with an all new ultra-stable, fully polarimetric 1.56 THz transceiver system a few years later[3]. Very recently, newly designed waveguide mounted heterodyne mixers were installed into a new ultra-stable, laser based, 325GHz transceiver system at STL[4]. The use of these heterodyne detectors increases the available dynamic range of sensitivity to around 170dB. The heterodyne detection systems in use also allow the complex scatterer back-reflection components (R, θ) or (I, Q) to be collected. Recently, terahertz laser systems have been used as local oscillator (LO) sources in remote areas for radio astronomy[5]. While the attainable frequency and power output of solid-state multiplier-chain devices is improving, they are presently too weak to be utilized as a local oscillator for a heterodyne detector. For now, the best source of milliwatt class terahertz radiation is a CO_2 laser pumped, far-infrared laser.

A typical measurement sequence conducted inside an STL Compact Radar Range would involve the use of a swept frequency source, usually a Schottky diode or waveguide mounted sideband generator. This sideband generator takes an RF signal and mixes it with the terahertz laser frequency to produce a new frequency at the base laser frequency plus the RF frequency. Positioning the target and collecting the backscattered data at a number of discreet frequency steps in a chirp of the outgoing laser allows post-collection generation of an Inverse Synthetic Aperture Radar (ISAR) image.

For the imagery and data collection described here, no frequency chirp was applied. The measurements collected for this work were a bit unusual to the typical ISAR measurement, in that these measurements consist of a single frequency measurement taken at numerous angular poses. Since the compact ranges were originally designed to accurately position the target object, rather than scan the actual far infrared beam, the measurements described produce imagery via controlled motion of the scan object. While this approach has little use in scanning live or moving objects, it is presented as an exercise for studying the terahertz phenomenology of complex scattering objects.

Following data collection, Fourier Transform (FT) or Fast Fourier Transform (FFT) processing of a series of the back-scattered values collected across a two dimensional angular aperture effectively convert the data into an angular Doppler Shifted image. This Doppler Shift image looks to the eye like the physical object being measured. Scattering centers reflected from the target of interest are represented via a false color Z-axis.

2. TERAHERTZ TRANSCEIVER SYSTEM

2.1. The Transmitter Source and Receivers

Many of the radar measurements at STL utilize the CO_2/FIR laser combination as the preferred source of terahertz radiation. While the output from the FIR laser is fairly narrowband for a chosen operating wavelength, it is currently the best source for high power (nominal 100mW) requirements requiring high stability.

Following many years of minor in-house improvements to commercial CO_2 and FIR laser designs, STL scientists and engineers set out to design an entirely new FIR laser, using information gleaned from years of operating commercially available CO_2 paired FIR lasers. The new FIR laser design included a balance of ease of use, nimbleness in controls, neutral cavity thermal expansion, and extremely low vacuum leak rate. The new FIR lasers were designed with thermal stability as a primary goal, with water jacketed tube bores and water cooled optics mounts. Because the FIR lasers used would potentially operate at frequencies anywhere from 50μm to 5000μm, the laser design allows the use of dielectric waveguide resonator tube bores over a wide range of diameters, as dictated by Eigenmode resonator design. Performance figures of these lasers show that after only a few hours of warm up time, the output power is very stable, and the phase stability is better than 10° in absolute phase in a 24 hour period.

With the great success of a more stable FIR laser, STL set out to improve on the CO_2 laser design, to produce a pump laser with more frequency stability. Pacific Research (Topanga, CA) delivered a custom CO_2 laser that proved to be extremely stable in power and frequency drift. With a typical output power of close to 200 watts continuous wave (CW) in the CO_2 laser, the resulting power levels produced by the far-infrared lasers are impressive, usually around 100 milliwatts. Our five Pacific Research CO_2 lasers have now become the standard optical pump laser for six operating STL FIR lasers.

The rotational/vibrational transition of the CO_2 molecule in the carbon dioxide laser provides a robust source of mid-infrared input power for the rotational transitions needed in the FIR laser. For a discreet CO_2 laser pump line, in a particular molecular gas, at a particular pressure, and in an optimally designed resonator, FIR power can be achieved with modest efficiencies of around 0.10%.

The measurements were performed on two entirely separate compact radar ranges at STL, each system consists of two CO_2/FIR laser pairs whose outputs are zero order transverse Gaussian modes. One CO_2/FIR is used to generate the transmit beam, and another is used to produce a local oscillator (LO) beam. The two beams produced are approximately 2 GHz apart, which requires each FIR laser to be pumped by it's own CO_2 laser, often requiring an entirely different molecular gas in the FIR laser. The 1.56 THz system uses the 1.5645 THz line in methanol (CH_3OH) gas for the transmitter, and the 1.5626 THz line in difluoromethane (CH_2F_2) for the LO. The 325 GHz

system uses the 325.9 GHz line for the transmit beam, and the 323.6 GHz line for the LO, both in O-deutero-formic acid (HCOOD) vapor.

The receivers in use on the two terahertz systems use both old and new technologies. The 1.56 THz receiver is a corner-cube mounted, whisker contacted Schottky diode, made originally by University of Virginia in the 1990's. The 1.56 THz system noise temperature is about 9000°K, with a conversion loss of 14 dB. The receivers for the 325 GHz system are relatively new technology, and use a freestanding waveguide mounted detector made by Virginia Diode (Charlottesville, VA). In the current 325 GHz system, they have a 1500°K system noise temperature and a system conversion loss of around 8.5 dB. Both heterodyne detectors enable the measurement systems to have a dynamic range of around 170 dB.

2.2. Anechoic Chamber and Data Collection System

Compact radar ranges in use at STL consist of a climate controlled room with materials specifically designed to absorb terahertz radiation (anechoic materials)[6] attached to all the walls in the room. The transceiver system sits just outside the anechoic chamber, and a small opening in the chamber allows the passage of the transmitted and back-reflected radiation. The outgoing beam, the transmit or illumination beam, is close to 24 inches in diameter at the full-width-half-maximum (FWHM), which fully illuminates the target object with a planar phase front. An overview of a typical laser based transceiver may be found in Figure 2.

To produce the aforementioned Angular Doppler imagery, commonly referred to as azimuth/elevation or "Az/El" imagery, a very accurate control over the motion of the scanned object is required. The positioning apparatus is located in the anechoic chamber, and the mechanical components are shielded from the illuminating beam. The target object sits atop the stepper motor positioning staging, which allows positioning accuracy on the order of 0.005 degrees in both the azimuth and elevation axis of motion. The azimuth axis stage allows full rotation of the object through 360 degrees. The elevation axis allows motion from 0 degrees, fully upright, to 90 degrees, where the scan object would be tilted full forward. The combination allows an entire hemisphere to be measured.

For each azimuth/elevation pose of the object, complex scatterer data is collected by way of a lock-in amplifier, which provides in-phase and quadrature (I,Q) values. The signals from the lock-in amplifier are acquired using National Instruments analog-to-digital hardware, controlled by custom designed LabVIEW® software.

3. DATA COLLECTION AND PROCESSING

3.1 Angular Doppler Data Collection Theory and Practice

The Angular Doppler imagery techniques are described in detail by Mensa,[7] the slight difference in implementation for this work involves use of a stationary transceiver, and a strictly two dimensional holographic recording of data. The target object to be measured is placed in the center of the terahertz laser transmitter beam. The resultant imagery produces pixel values in a coordinate system of vertical and horizontal cross-range, corresponding to a two dimensional matrix of amplitude values.

For the azimuth axis, it is convenient to place the object centered about the axis of rotation. The object is revolved around the azimuth axis, and complex (I, Q) pairs are collected at evenly spaced intervals. To add a second dimension to the image, a similar collection is performed in the elevation axis. A two-dimensional scan would consist of an azimuth sweep, followed by an elevational increment, and the process would repeat until a two dimensional "window" is swept out in angle. A complex Fourier Transform can then performed on this data, to generate coordinate values as a function of phase change between angular increments as shown in Figure 3, a scatterer that is some radius from the center of azimuth rotation will change the received phase value as the object is moved in azimuth. The phase change corresponds only to motion perpendicular to the illuminating beam's phase front. A positive change in phase between two successive azimuth positions would correspond to a motion moving towards the receiver, while a negative phase change would correspond to motion away from the receiver. By Fourier Transforming a number of these positions, the phase change trend can be extracted in the conversion from spatial frequency to distance. The displayed plot in Figure 4 shows the Fourier transform of 512 points collected in a single azimuth scan. Values to right of center are objects moving towards the receiver, objects to the left of center are

moving away from the receiver, and the center of the plot shows zero phase change, no movement with respect to the receiver. The X-axis of the plot in Figure 4 shows the spatial frequency Doppler shift transformed into horizontal distance from the center of rotation. With a few simple conversion calculations, the x-axis may be assigned convenient units of distance.

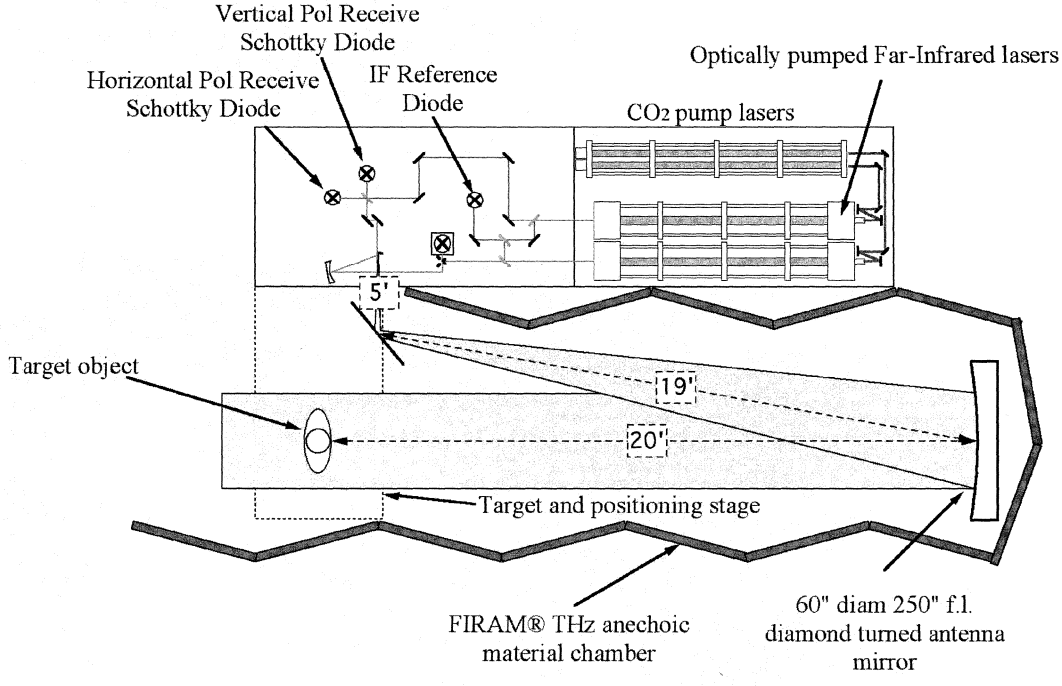

Figure 2. Schematic of a laser based terahertz transceiver at STL.

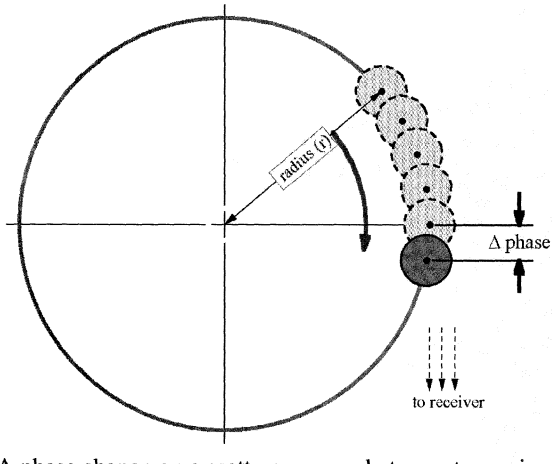

Figure 3. A phase change on a scatterer occurs between two azimuth positions.

To ensure proper sampling of the azimuth points and to prevent under-sampling, Equation 1 must be used to determine the unambiguous cross-range and the maximum diameter of the object to be scanned. For the

calculated diameter, the change in phase at the edges corresponds to 90 degrees. A phase change greater than 90 degrees between points becomes ambiguous, that is, it is not possible to determine which direction in which the Doppler shift occurred. The result would produce a corrupt "folded" image, where anything outside the unambiguous cross range would look folded in at the edges. Larger scan objects would require a finer scan resolution, smaller objects can afford a more coarse scan resolution.

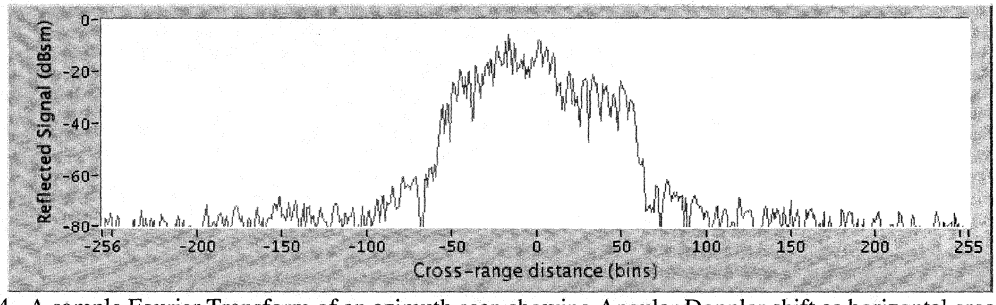

Figure 4. A sample Fourier Transform of an azimuth scan showing Angular Doppler shift as horizontal cross-range.

The elevation axis calculations are similar in unambiguous cross-range, but for generating the following images, the object was above the axis of rotation in the elevation direction. An unfortunate artifact of the data collection and processing exists at the zero azimuth, zero elevation location, corresponding to all signals that did not change in the duration of the scan. This small grouping for pixels in the 2D image shows the amplitude for all noise and background signals in the system. In order to prevent these pixels from appearing in the center of the terahertz image, the object is mounted such that the elevation axis is below the scan object. In the final imagery the lower part of the image, that which corresponds to objects moving away from the receiver, is removed by cropping the image.

(1) $$R_u = \lambda / 2\theta_{inc}$$

To calculate the pixel size as a function of the angular extent of the FT processing, Equation 2 may be used. Through a simple equation manipulation, a desired pixel size could also be used to determine the required angular extent to process.

(2) $$\Delta R_c = \lambda / 2\Delta\theta_{integrated}$$

For the imagery formed at 325 GHz and 1.56 THz, the integrated angle was kept fairly small, under 10 degrees, to prevent blurring or smearing of the imagery. As the integrated angle becomes large, phase focusing algorithms are needed to compensate for horizontal motion as the object traces out the curvature of the azimuth pivot. Because the data presented here is processed over relatively small angles, the phase focusing need not be applied.

4. RESULTS

Results of the two-dimensional data collection and data processing are shown below. The amplitude (Z-axis) values are shown in a false color "rainbow". Values in red are the most intense, moving down in amplitude of back-scatter to orange, yellow, green, blue, and purple. As the amplitude drops below a threshold value, the color goes to black, allowing the background to threshold all the very low level residual noise. Preliminary measurements were performed on $1/16^{th}$ scale models of vehicles, readily available in-house at STL. It is interesting to also note that because all dielectric materials on the models are modeled to simulate W-Band radar at 94 GHz, the terahertz images taken at 1.56 THz simulate true 94 GHz imagery of the full scale target. Figure 5 shows a 1.56 THz Az/El image of a $1/16^{th}$ scale model of a truck. The upper display is the false color imagery, and the lower display shows a photograph of the model. The apple in the photograph is to show the relative size of the model. The pixel resolution in the image is around 1.1mm square, corresponding to an FT integrated angle of 5.12 degrees in both azimuth and elevation.

The image on the left of Figure 6 shows the 1.56 THz imagery of a 4" square aluminum plate with raised letters "STL" and the words "University of Massachusetts" and "Submillimeter-Wave Technology Laboratory" wrapped along a circle above and below the center. On the right of Figure 6 is a photograph of the metal plate.

With the recent concerns of Homeland Security, and the recent scientific interest in manipulating terahertz waves, an attempt was made to image a concealed weapon through several layers of clothing. A mannequin was dressed in a cotton Tee shirt and a cotton jacket. The mannequin serves only to support the clothing material. The mannequin torso is a commercially available model, and no effort was made to replicate human skin. The mannequin is composed of a painted fiberglass form that is hollow, and has metal reinforcing material distributed throughout the torso for structural strength.

The image in Figure 7 shows a 1.56 THz image of a mannequin torso wearing a cotton jacket, with a gun object placed in an inside breast pocket of the jacket. The outline of the mannequin torso is a bit difficult to see, but the mannequin is facing directly towards the receiver (and the viewer) the head is not visible, but the shoulders and sides of the torso can be seen, down to about the elbows. The gun is clearly visible through the jacket, with good contrast against the mannequin.

The imagery in Figure 8 is the same mannequin with the same concealed weapon, in the same pose, but at 325 GHz. Here the contrast of the weapon seems to be reduced. The mannequin is constructed of a fiberglass and metal mesh, and since the wavelength of a 325 GHz beam is on the order of 920μm, it is believed that there is actually too much penetration through the clothing material. The 325 GHz beam is believed to be penetrating the fiberglass shell and reflecting around inside the hollow torso cavity. The measurement can therefore not be used as a true representation of measuring a human with a concealed weapon. Additional studies must be performed to assess the properties of a live object with skin and flesh.

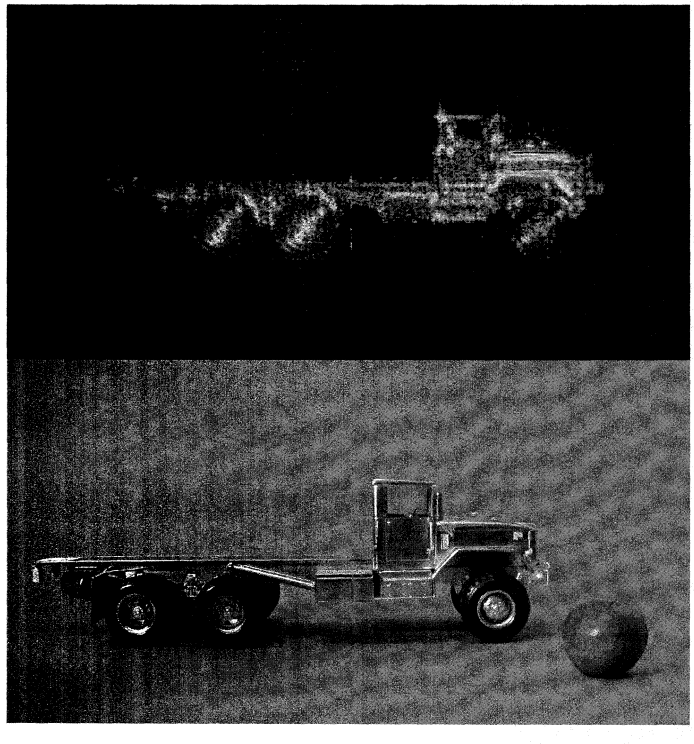

Figure 5. 1.56 THz Azimuth/Elevation imagery of a scale model truck with pixel resolution of about 1.1mm x 1.1mm.

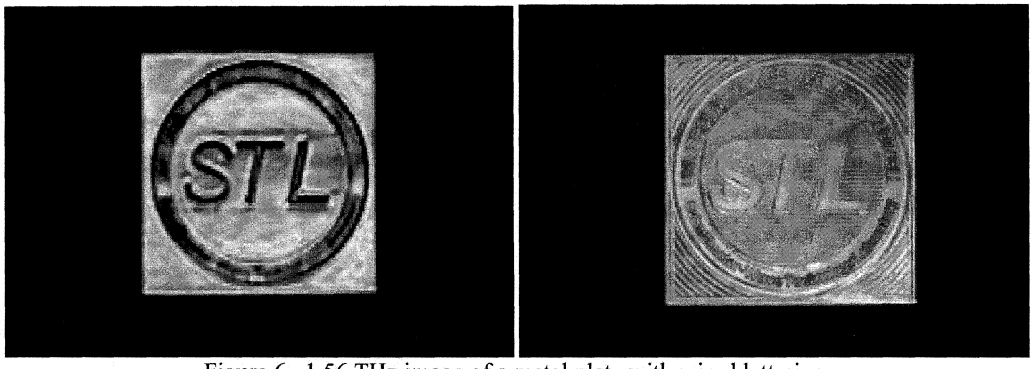

Figure 6. 1.56 THz image of a metal plate with raised lettering.

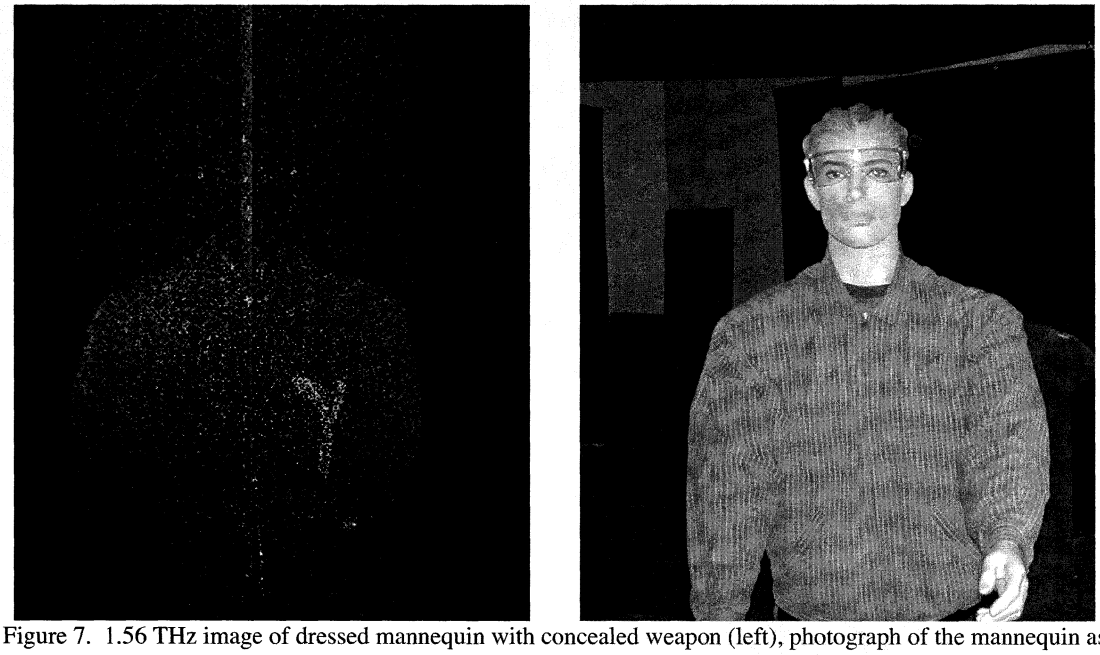

Figure 7. 1.56 THz image of dressed mannequin with concealed weapon (left), photograph of the mannequin as measured (right).

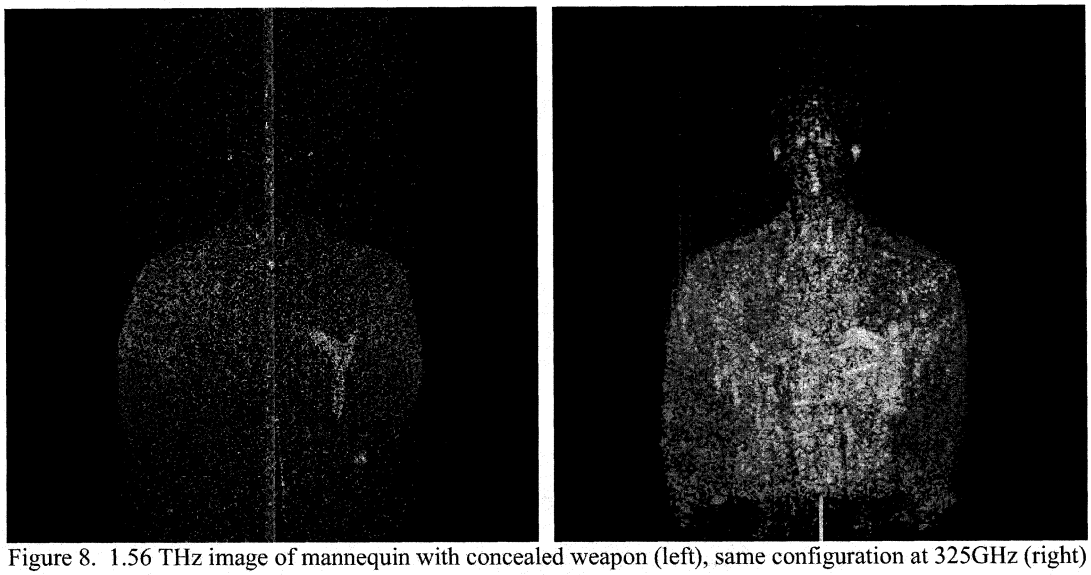

Figure 8. 1.56 THz image of mannequin with concealed weapon (left), same configuration at 325GHz (right)

5. SUMMARY

Terahertz images of several objects were produced, using a technique borrowed from the radar community. The images shown were collected at 1.56 THz and 325 GHz (0.325 THz). Both terahertz transceiver systems used a fixed position transmitter and receiver, and the scan object was moved in a precise motion through a series of angles. By two dimensional Fourier Transform post-processing, the data collected over an angular window in the azimuth axis and the elevation axis, forms a two dimensional image of variable resolution and very high sensitivity.

6. REFERENCES

1. J. Waldman, H. R. Fetterman, W. D. Goodhue, T. G. Bryant, D. H. Temme,"**Submillimeter Modeling of Millimeter Radar Systems**", SPIE Proceedings on Millimeter Optics , Vol. 259, p. 152 (1980).

2. E.R. Mueller, and J. Waldman,"**Power and Spatial Mode Measurements of a Sideband Generator Submillimeter-Wave Source**", Proceedings of the Eighth International Symposium on Space Terahertz Technology, Cambridge, MA, March 1997

3. Thomas M. Goyette, Jason C. Dickinson, William J. Gorveatt, Jerry Waldman, William E. Nixon,"**X-Band ISAR Imagery of Scale Model Tactical Targets Using a Wide Bandwidth 350GHz Compact Range**", SPIE AeroSense Conference. 12 - 16 April 2004, Orlando, Florida

4. Thomas M. Goyette, Jason C. Dickinson, Jerry Waldman, William E. Nixon,"**Three Dimensional Fully Polarimetric W-band ISAR Imagery of Scale-Model Tactical Targets Using a 1.56 THz Compact Range**", SPIE AeroSense Conference. 21 - 25 April 2003, Orlando, Florida

5. K.S. Yngvesson, C.F. Musante, M. Ji, F. Rodriguez, Y. Zhuang, E. Gerecht, M. Coulombe, J. Dickinson, T. Goyette, J. Waldman, C.R. Walker, A. Stark, and A. Lane,"**Terahertz Receiver With NB/N Device (TREND) - A Low-Noise Receiver User Instrument For AST/RO at the South Pole**", Proceedings of the 12th International Symposium on Space Terahertz Technology, California Institute of Technology, Pasadena CA, March 2001.

6. R.H. Giles, T.M. Horgan, and J. Waldman,"**Silicon-Based Anechoics at Terahertz Frequencies**", Proc. of the 17th Int. Conf. on Infrared and Millimeter Wave , Dec. 1992, Los Angeles, CA.

7. D.L. Mensa, *High Resolution Radar Cross-Section Imaging*, Artech House, Boston, MA 1991.